



## Research paper

# Impact of mixing design parameters on the performance and surface quality of self-compacting concrete filling layers

Jingyi Zhang<sup>1</sup>, He Liu<sup>2</sup>, Ji Zhang<sup>3</sup>

**Abstract:** Construction quality, durability and service life of China Railway Track System III (CRTS III) is influenced by the performance of the self-compacting concrete (SCC) used for filling layer. In this paper, the effect of unit water consumption, sand ratio and water reducer components on working performance of SCC filling layer is studied by laboratory and field tests. Appropriate mix proportion parameters are obtained. The results indicate that unit water consumption can significantly improve the in-service performance of SCC. However, it is essential to consider both the dosage of water-reducing agents and the unit water consumption to ensure the stability of the mixture. Sand ratio of SCC is between 49% and 52% used for filling layer, which have excellent flowability and stability. It is recommended that the content of the defoamer should be 3/1 000, and the content of the air-entraining agent should be 5/1000. These research results will play an important role in improving the construction quality of SCC filling layer

**Keywords:** self-compacting concrete, mix proportion parameters, laboratory test, field test, surface quality

<sup>1</sup>M. Eng., Shenyang Urban Construction University, School of Civil Engineering, No.380 Bai Ta Road, Hunnan, e-mail: [dq\\_zjy@syucu.edu.cn](mailto:dq_zjy@syucu.edu.cn), ORCID: 0000-0003-4641-5191

<sup>2</sup>PhD., Eng., Shenyang Jianzhu University, School of Transportation and Geomatics Engineering, No. 25 Hunnan Zhong Road, Hunnan District, Shenyang, Liao Ning, 110168, China, e-mail: [helu@sjzu.edu.cn](mailto:helu@sjzu.edu.cn), ORCID: 0000-0002-3867-0726

<sup>3</sup>M. Eng., Liaoning New Development Highway Technology Maintenance Co., LTD, Shenyang, Liaoning, 110000, China, e-mail: [13324131953@163.com](mailto:13324131953@163.com), ORCID: 0009-0005-8086-3846

## 1. Introduction

The CRTS III slab ballastless track system (CRTS III), independently developed by Chinese railway companies, is utilized in high-speed railway construction [1]. SCC filling layer is a critical structural component of the CRTS III [2, 3]. The track structure consists of four layers: prefabricated prestressed slab, filling layer, geotextile layer, and base plate, as shown in Fig. 1 [4]. SCC filling layer is a huge panel structure with a typical dimension of 90 mm thickness, 2500 mm width, and 5600 mm length. According to design principle, it's that SCC filling layer is required to display strong bonding with the above steam-cured concrete prefabricated slab. The loads of the high-speed train are transferred to the roadbed by the composite plate. The interface bonding between prefabricated track slab and filling layer should be strong bonding and durable enough to ensure serviceability of the slab track [5]. Bleeding, rising of bubbles and foaming layer should be strictly controlled. Moreover, SCC is cast into the sealed filling layer from the pouring hole, as shown in Fig. 2. SCC used for filling layer of CRTS III is required to fill up the sealed space between slab and base plate by its own weight without any vibration. Compared to normal SCC, SCC used for slab track system flows on a flexible geotextile and flows through steel mesh. It increases the flow resistance. Filling layer structure is sealed space. Top surface of SCC filling layer can't be smoothed by the process of finishing. Same defects such as bleeding, rising of bubbles and foaming layer aren't acceptable [6]. Furthermore, some defects often appear on the surface of filling layer in filling layer construction process. Bonding interface between track slab and filling layer will be destroyed extremely by defects under continuous dynamic loading [7–9]. Even comfortable, safety and service life of track system will be influenced by effects. Therefore, the influence of SCC mix proportion parameters on SCC performance and surface quality for filling layer should be further studied.

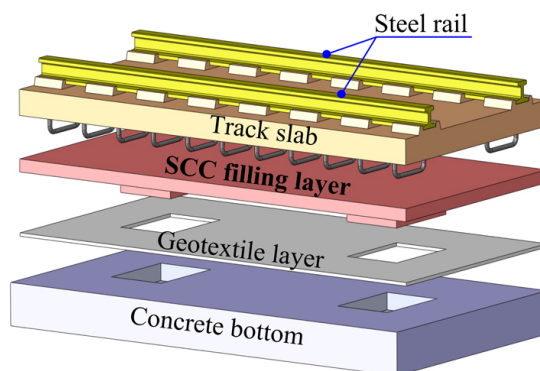


Fig. 1. Schematic diagram of slab track structure

Researchers focused on working performance of SCC [10–22]. The working performance of SCC included fluidity, filling ability, passing ability, and segregation resistance. Related research results showed that reducing aggregate volume could increase the fluidity of SCC [10, 11]. With fine aggregate to total aggregate weight ratio increase, the slump flow of SCC decreased

consistently [12]. Segregation tendency of SCC with lightweight aggregate content increase was increased [13]. High and low water to cement ratios may be caused segregation or blocking of SCC [14]. Fibers had significant effect on SCC workability. Filling ability, passing ability and self-compacting ability of SCC decreased with carbon fiber volume fraction increase [15, 16]. The effect of cementitious materials on working performance was revealed. Rheological properties and filling ability of SCC were enhanced by fly ash and slag [17, 18]. Filling ability of SCC was decreased with silica fume content increase [18]. The defoaming agent can reduce the proportion of large entrained air bubbles and enhance the stability of the remaining air bubbles [19]. The use of air entraining agent produced a large number of tiny bubbles, which increased total surface area of bubbles. These tiny bubbles could reduce the internal friction of SCC, result that flowing ability of SCC was enhanced [20]. Many researchers paid attention on quality and durability of SCC filling layer. Peng proposed impulse response method to detect the defect of SCC filling layer [23]. Slump-flow test of SCC for filling layer was simulated in 3D by the discrete element method [24]. Damage behaviors of SCC for filling layer was researched by three point bending tests [25]. The deformation mechanism and influencing factors of the track slab during the SCC casting process was revealed [26]. Relationship between apparent morphology of crushed stone aggregates and quality of SCC filling layer was proposed by field experiment [27]. Although many research results about SCC workability, quality and durability were proposed. There is lack of research on the relationship between SCC performance and surface quality for filling layer.

Thus, in this paper, according to the composition characteristics of SCC for filling layer, the influence of mix proportion parameters such as unit water consumption, sand ratio, deforming agent and air-reducing agent content on the workability of SCC for filling layer were studied. The relationship between mix proportion parameters of SCC and the surface quality of filling layer was analyzed by laboratory and field tests. Then, the appropriate mix proportion parameters were obtained. These research results will play an important role in improving the construction quality of SCC filling layer.

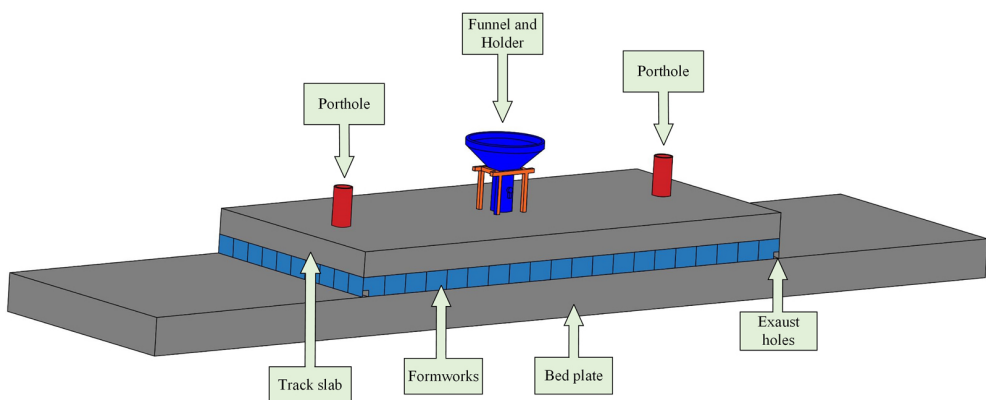


Fig. 2. Cast concrete from the top pouring hole

## 2. Experimental program

### 2.1. Materials

Ordinary Portland cement (C) used by Chinese standards GB175-2007 (GB 2007) with 28 days compressive strength over 42.5 MPa. Class I fly ash (FA) and ground granular furnace blast slag (GGBS) were used as mineral admixtures. The physical properties and chemical compositions of C, FA, GGBS are shown in Table 1. A calcium sulfoaluminate-based expansive agent (UEA) was used to make the mixture attaining a certain expansion. River sand (S) with a fineness modulus of 2.45 was used as fine aggregate. Its apparent density is 2650 kg/m<sup>3</sup>. The particle size of coarse aggregate (G) is 5–16 mm and its apparent density is 2745 kg/m<sup>3</sup>. The gradation curve of coarse aggregate and sand is shown in Fig. 3. The cellulose polymer and inorganic ultrafine calcareous and siliceous powder were used as viscosity modifying admixture (VMA) to improve mixture viscosity. Polycarboxylic acid superplasticizer (SP) with the water-reducing rate of 30% was used. Air-entraining agent was akyl-aryl sulfonate compound. Defoamer agent was polyalkylene glycol derivative. Tap water (W) was used as mixing water.

Table 1. Physical properties and chemical composition of C, FA, GGBS, (by wt%)

No.	SiO <sub>2</sub>	Al <sub>2</sub> O <sub>3</sub>	Fe <sub>2</sub> O <sub>3</sub>	CaO	MgO	SO <sub>3</sub>	Na <sub>2</sub> O +K <sub>2</sub> O -eq	Los on ignition	Specific surface area (m <sup>2</sup> /kg)	Apparent density g/cm <sup>3</sup>
C	24.6	7.30	4.00	59.7	3.8	2.5	0.60	2.50	350	3.12
FA	52.3	26.3	9.70	3.70	1.20	1.20	1.80	4.70	450	2.45
GGBS	26.1	13.8	14.1	33.6	8.10	–	0.45	2.10	420	2.87

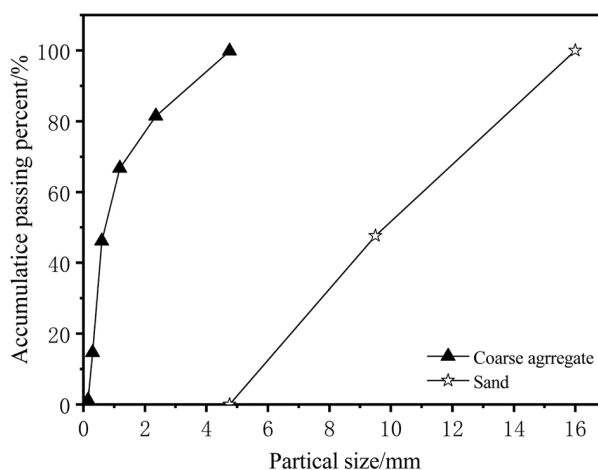


Fig. 3. The gradation curve of coarse aggregate

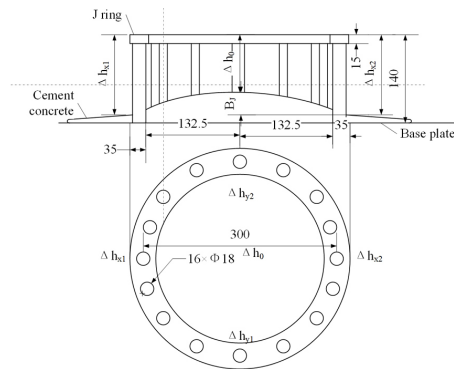
## 2.2. Testing methods

### 2.2.1. Laboratory test

In this experiment, seven groups of SCC mix proportions with different unit water consumption were performed, mixture numbers 1–7, as shown in Table 2. Seven groups of SCC mix proportions with different sand ratios were performed, mixture numbers 8–14, as shown in Table 2. Two groups of SCC mix proportions with different deforming agent and air-entraining agent contents were performed, mixture numbers 15–16, as shown in Table 2. Slump flow (SF),  $T_{500}$  time (The time it takes for self-compacting concrete to expand to 500mm), passing ability ( $B_J$ ) were tested according to JGJ/T283-2012, test pictures as shown in Fig. 4,  $B_J$  was calculated by Eq. (2.1).



(a)



(b)

Fig. 4. Pictures of slump flow and Passing ability: (a) Slump flow; (b) Passing ability

$$(2.1) \quad B_J = \frac{(\Delta h_{x1} + \Delta h_{x2} + \Delta h_{y1} + \Delta h_{y2})}{4} - \Delta h_0$$

$B_J$  – passing ability ( $J$  – ring blocking step), mm,

$\Delta h_{x1}$ ,  $\Delta h_{x2}$ ,  $\Delta h_{y1}$ ,  $\Delta h_{y2}$  – height difference between the top surface of concrete and the top surface of  $J$  ring in the direction of  $x$  axis and  $y$  axis of the outer edge of  $J$  ring,

$\Delta h_{x0}$  – height difference between the top of concrete and the top of  $J$  ring at the center of  $J$  ring.

The stability index  $L$  was determined by measuring the thickness of top surface paste. Thickness of the top surface paste was measured by self-designed device, as shown in Fig. 5. Device consists three parts, steel sheet testing cross, cylindrical container; and bracket. In this test, fresh SCC was casted into a cylindrical container with a height of 110 mm and diameter of 200 mm, and waiting for 15 min. Afterwards, the steel sheet cross with thickness of 1 mm, length of 150 mm, and height of 10 mm was fixed right on top of the concrete's surface. The steel sheet testing cross (A1) was quickly loosened, and finally measurements the going down depth of the cross were taken within 30 s. It is believed that the surface paste thickness test is sensitive enough to evaluate the segregation degree of fresh SCC. The segregation resistance is very good and acceptable when the  $L$  index no more than 7.5 mm, which is approximately equal to the thickness of mortar layer enveloped coarse aggregate [28].

Table 2. Mix proportioning of SCC

No.	C /kg	FA /kg	GGBS /kg	UEA /kg	VMA /kg	S /kg	G /kg	W /kg	SP /kg	Defoaming agent/% <sub>cc</sub>	Air- entraining agent/% <sub>cc</sub>	Sand /ratio/% <sub>c</sub>
1	325	70	60	45	30	807	807	170	7.72	–	–	50
2	325	70	60	45	30	807	807	172	7.72	–	–	50
3	325	70	60	45	30	807	807	174	7.72	–	–	50
4	325	70	60	45	30	807	807	176	7.72	–	–	50
5	325	70	60	45	30	807	807	178	7.72	–	–	50
6	325	70	60	45	30	807	807	180	7.72	–	–	50
7	325	70	60	45	30	807	807	182	7.72	–	–	50
8	335	40	80	45	30	759	856	174	7.42	–	–	47
9	335	40	80	45	30	791	823	174	7.42	–	–	49
10	335	40	80	45	30	807	807	174	7.42	–	–	50
12	335	40	80	45	30	807	775	174	7.42	–	–	51
13	335	40	80	45	30	839	774	174	7.42	–	–	52
14	335	40	80	45	30	872	743	174	7.42	–	–	54
15	335	40	80	45	30	807	807	174	7.42	3	–	50
16	335	40	80	45	30	807	807	174	7.42	3	5	50

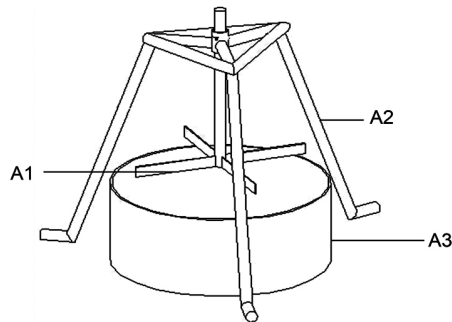


Fig. 5. Schematic diagram of top surface paste thickness measurement: A1 – represents the steel sheet testing cross; A2 – expresses cylindrical container; A3 – the bracket

### 2.2.2. Field tests

The construction process of filling layer is shown in Fig. 6. The construction process mainly includes four steps. In the first step, the bottom plate, geotextile layer and reinforcement mesh were installed from bottom to top, as shown in Fig. 6(a). In the second step, the prefabricated slab was hoisted to the top of base plate and installed to the design position, as shown in Fig. 6(b). In the third step, the space between the base plate and slab was sealed, the position of the slab was fixed by the clamps, as shown in Fig. 6(c). In the fourth step, SCC was poured from the pouring hole into a sealed space through the funnel, as shown in Fig. 6(d). According to the above steps, the fresh SCC with different unit water consumption, sand ratio, and water reducing agent components were tested. In the test, the quality of SCC could be visually judged by the observation from exhaust holes. Exposing plate test was carried out after pouring process finishing 24 hours later. The surface quality of SCC filling layer was judged by observation.



Fig. 6. The main construction steps of CRTS III slab ballastless track

### 3. Results and discussion

#### 3.1. Unite water consumption

The relationship between unit water consumption and SCC workability indexes is shown in Fig. 7. Compared with unit water consumption was  $170 \text{ kg/m}^3$ , when unit water consumption was  $172 \text{ kg/m}^3$ ,  $174 \text{ kg/m}^3$ ,  $176 \text{ kg/m}^3$ ,  $178 \text{ kg/m}^3$ ,  $180 \text{ kg/m}^3$ ,  $182 \text{ kg/m}^3$ , SF increases about 4.1%, 7.9%, 8.2%, 10.7%, 11.5%, 13.1%,  $T_{500}$  time decreases about 10.8%, 29.2%, 35.4%, 41.5%, 47.7%, 55.4%, passing ability increased about 21.4%, 28.6%, 45.7%, 42.9%, 85.7%, 157.1%, and stability index  $L$  increased about 123.1%, 169.2%, 269.2%, 438.5%, 669.2%, 1053.8%, respectively. It can be observed that SF, passing ability, and stability index  $L$  increased significantly, and  $T_{500}$  time decreased significantly with the increase of unit water consumption.

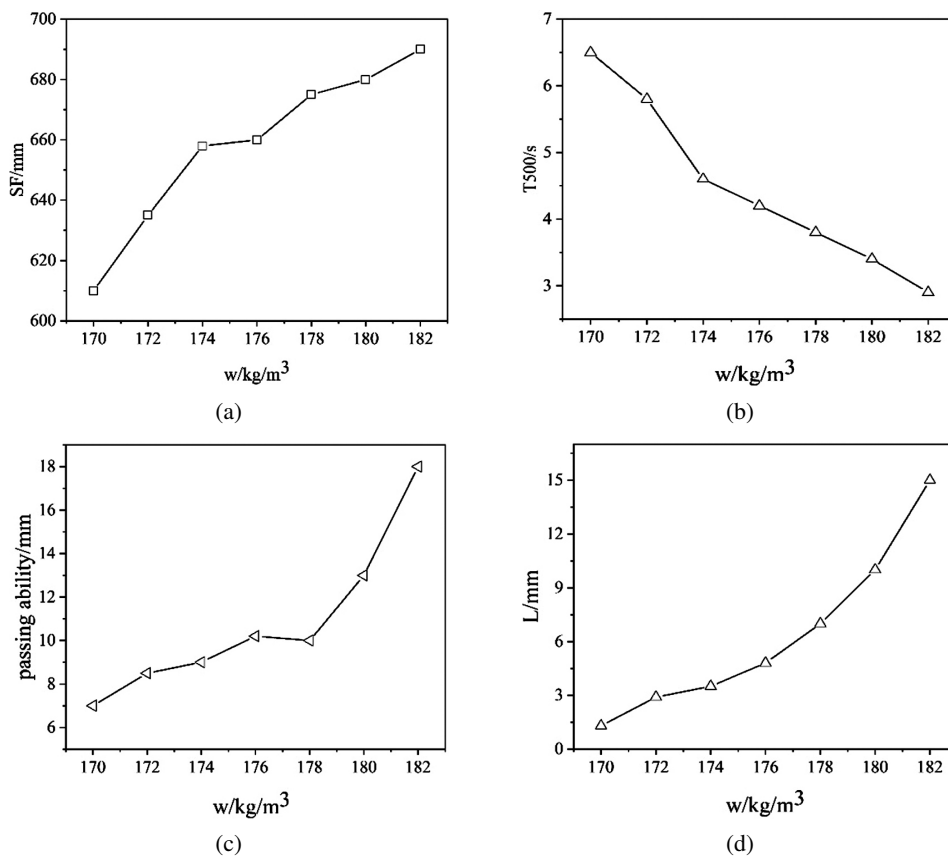


Fig. 7. Relationship between unit water consumption and SCC workability indexes: (a) SF; (b)  $T_{500}$ ; (c) passing ability; (d)  $L$

When the unit water consumption was  $170 \text{ kg/m}^3$ , SF is 610 mm,  $T_{500}$  time is 6.5 s. Flowability of SCC is poor. When unit water consumption increased from  $170 \text{ kg/m}^3$  to  $172 \text{ kg/m}^3$ ,  $174 \text{ kg/m}^3$ ,  $176 \text{ kg/m}^3$ ,  $178 \text{ kg/m}^3$ , SF and passing ability of SCC increased,  $T_{500}$  time decreased, and the SCC showed good flowability. However, with the further increase of unit water consumption, when unit water consumption was  $180 \text{ kg/m}^3$  and  $182 \text{ kg/m}^3$ , the stability index  $L$  increased significantly and more than 7.5 mm, SCC showed segregation phenomenon.

At the same time, when unit water consumption was  $170 \text{ kg/m}^3$ , SCC showed poor fluidity, which led to the unfilled phenomenon of SCC filling layer, as shown in Fig. 8(a). When unit water consumption was too large, large bubbles and laitance layer on the filling layer surface was observed, as shown in Fig. 8(b).



Fig. 8. Surface quality of SCC filling layer: (a)  $170 \text{ kg/m}^3$ ; (b)  $182 \text{ kg/m}^3$

### 3.2. Sand ratio

The relationship between sand ratio and SCC performances are shown in Fig. 9. Compared with 47% sand ratio, when sand ratios were 48%, 49%, 50%, 52%, 54%, SF decreased about 2.8%, 3.5%, 6.3%, 12.7%,  $T_{500}$  increases about 24%, 56%, 68%, 132%, passing ability decreased 25.8%, 41.2%, 59.9%, 65.9%, stability index  $L$  decreased about 30.1%, 48.5%, 62.1%, 77.7%, respectively. It can be observed that with the increase of sand ratio, SF, passing ability, and stability index  $L$  decreased,  $T_{500}$  time increased continuously. The main reason is that the increase of sand volume content leads to the increase of viscosity and yield stress of the mortar system, which leads to SF and passing ability of SCC decrease,  $T_{500}$  time increase, and stability index  $L$  decreases significantly. The stability index  $L$  decreases significantly, which indicates that SCC stability is increased.

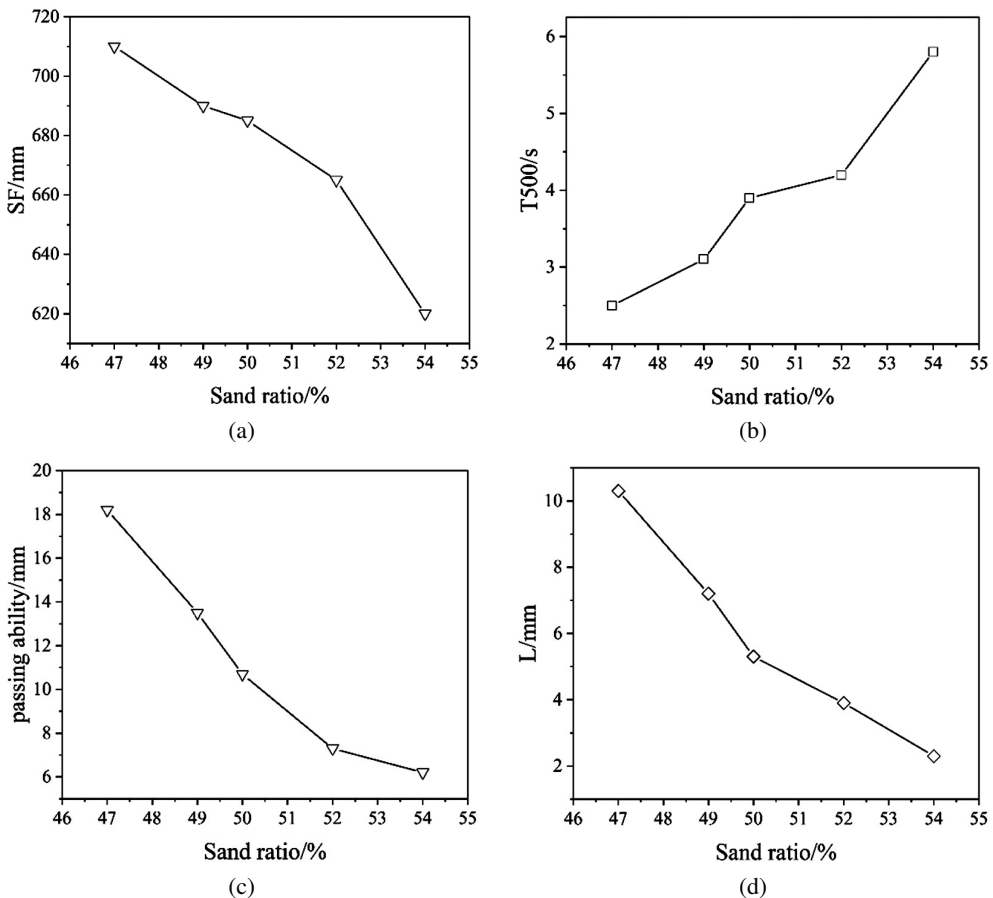


Fig. 9. Relationship between sand ratio and SCC performance index: (a) SF; (b)  $T_{500}$ ; (c) passing ability; (d)  $L$

In this paper, combined with the field tests, the state of vent concrete and surface quality of filling layer SCC with sand ratios of 47%, 52%, and 54% were analyzed. As shown in Fig. 10(a), 47% sand ratio of SCC flowed out of the vent with less aggregate content. The reason is that the sand ratio is too low, which results in low viscosity value of the mortar system and weakens the ability of the mortar to transport aggregate. Also, as shown in Fig. 9(d), the stability index  $L$  was more than 7.5 mm, the SCC with poor stability, which can explain the above result. This phenomenon will lead to segregation of the filling layer SCC and affect its service performance. At the same time, due to segregation, shrinkage stress distribution of SCC is inconformity, which results the stress concentration, it further development will lead to shrinkage crack of SCC filling layer. The surface quality of filling layer is shown in Fig. 10(b). It can be seen that along concrete flow direction with many big diameter bubbles on surface of SCC filling layer. At the same time, there were laitance layer on the surface of filling layer.

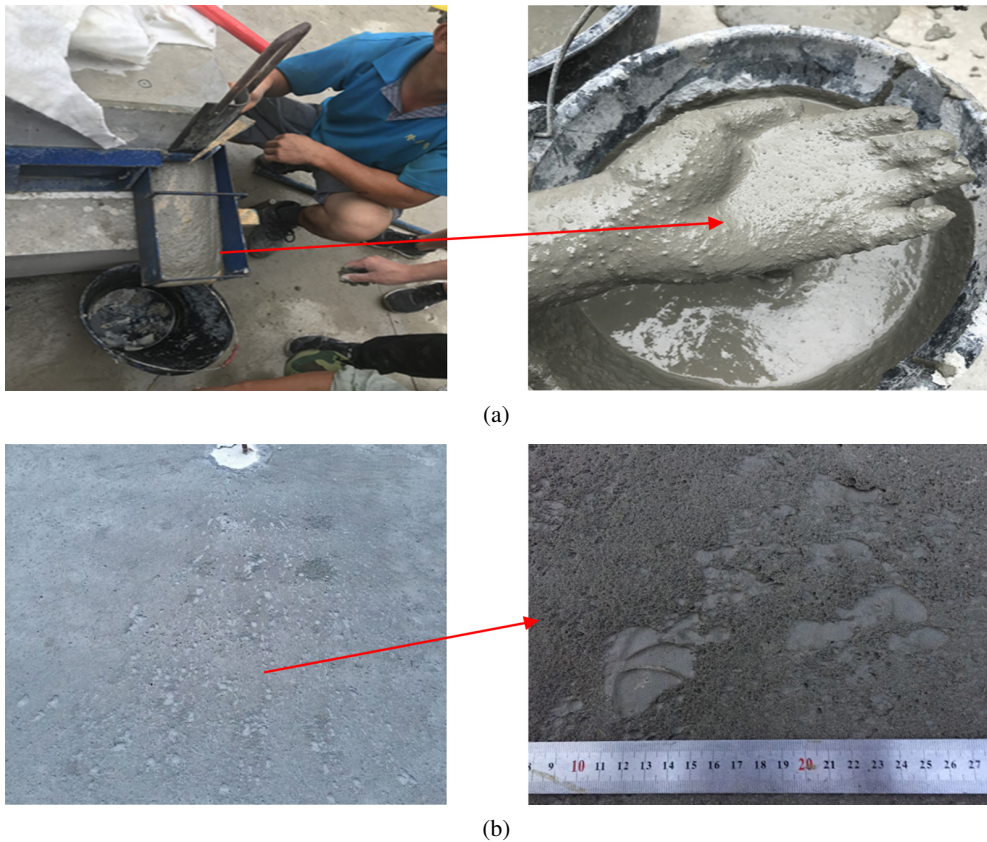


Fig. 10. Effect of 47% sand ratio on the quality of vent concrete and filling layer: (a) State of vent concrete; (b) Surface quality of filling layer

The SCC with a sand ratio of 50% showed good homogeneity, and the mortar-wrapped stones uniformly flowed out, as shown in Fig. 11(a). At the same time, the surface quality of filling layer was in a good condition, and large bubbles and laitance layer was not observed, as shown in Fig. 11(b). It can be seen that with the increase of sand ratio, the stability of SCC can be effectively improved.

The SCC with a sand ratio of 54% was used for the plate filling test. As shown in Fig. 12, there were many long and narrow bubbles around the filling layer, which were perpendicular to the SCC flow direction. It indicates that when the sand ratio is too large, although the stability of SCC is good, the loss of flow performance is too large. It will lead to residual paste volume being too small to lose the self-healing ability. Therefore, when this SCC flows to the surrounding formwork, the air in the plate cavity cannot be completely discharged without enough residual paste.



Fig. 11. Effect of 50% sand ratio on the quality of vent concrete; (a) State of vent concrete; (b) Surface quality of filling layer



Fig. 12. Effect of 54% sand ratio on the quality of filling layer

### 3.3. Water reducer components

When the SCC paste had a suitable viscosity, due to the excessive amount of defoaming agent in the water reducing agent, there were more bubbles floating on the surface of fresh SCC as shown in Fig. 13(a). At the same time, more circular bubbles appeared on the surface of the filling layer, as shown in Fig. 13(b). When the combination point of defoamer content and air-entraining agent content were found, the fresh SCC was put into the bucket car, then with face closure. After 10 minutes of rest, there were no bubbles floating on the concrete surface, as shown in Fig. 13(c). After pouring the SCC and uncovering the plate, there were fewer bubbles on the surface, as shown in Fig. 13(d).

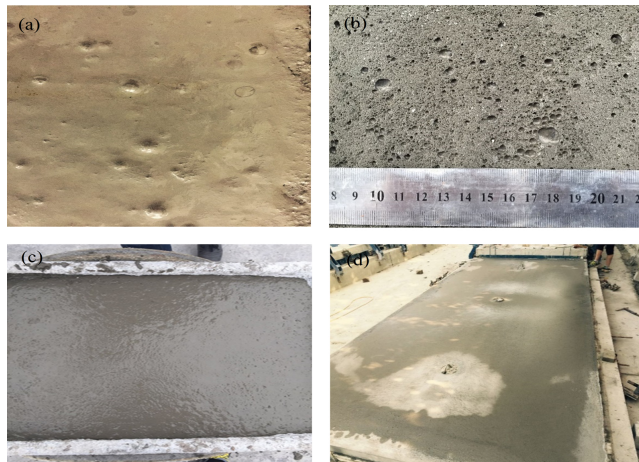


Fig. 13. Effect of water reducer components on the quality of filling layer: (a) Effect of excess defoamer on surface bubbles of SCC; (b) Effect of excessive defoamer on surface quality of filling layer; (c) Effect of suitable defoamer and air-entraining agent on surface bubbles of SCC; (d) Effect of suitable defoamer and air-entraining agent on bubble state of filling layer

## 4. Conclusions

In this paper, influence of mix proportion parameters on self-compacting concrete performance and surface quality for filling layer was studied. Based on the above experiments, the following conclusions can be drawn.

(1) Unit water consumption can significantly improve the working performance of SCC, but it is necessary to comprehensively consider the dosage of water reducing agent and unit water consumption to ensure its stability.

(2) Sand ratio of SCC in the filling layer is between 49% and 52%, which can have excellent flowability and stability.

(3) The filling layer SCC can improve the stability of SCC bubbles by using the method of “first elimination and then introduction.” In this paper, it is recommended that the content of the defoamer should be 3/1 000, and the content of the air-entraining agent should be 5/1000. At the same time, in different cementitious systems, the binding points of defoamer and air-entraining agent content are different, which need to be determined through laboratory tests and uncover panel tests.

## Acknowledgements

This work was supported by basic scientific research project of Liaoning Education Department (grant number: LJKMZ20221928); Liaoning transportation technology project (grant number: 202328).

## References

- [1] Q. Yuan, et al., “Sealed-space-filling SCC: A special SCC applied in high-speed rail of China”, *Construction and Building Materials*, vol. 124, pp. 167–176, 2016, doi: [10.1016/j.conbuildmat.2016.07.093](https://doi.org/10.1016/j.conbuildmat.2016.07.093).
- [2] H. Liu, et al., “Investigation on mechanical behaviors of Self-compacting concrete containing reclaimed asphalt pavement”, *Construction and Building Materials*, vol. 346, art. no. 128421, 2022, doi: [10.1016/j.conbuildmat.2022.128421](https://doi.org/10.1016/j.conbuildmat.2022.128421).
- [3] H. Liu, G.C. Duan, F.C. Wang, J.Y. Zhang, J. Zhang, and Y. Guo, “Numerical simulation of effect of reclaimed asphalt pavement on damage evolution behavior of self-compacting concrete under compressive loading”, *Construction and Building Materials*, vol. 395, art. no. 132323, 2023, doi: [10.1016/j.conbuildmat.2023.132323](https://doi.org/10.1016/j.conbuildmat.2023.132323).
- [4] W. Li, K.L. Ma, G.C. Long, N. Li, L.S. Yu, and Q.Q. Xie, “Influence of workability parameters and filling time on the quality of SCC filling layers”, *Magazine of Concrete Research*, vol. 73, no. 12, pp. 636–647, 2021, doi: [10.1680/jmacr.19.00342](https://doi.org/10.1680/jmacr.19.00342).
- [5] Z.H. Zheng, L. Liu, P. Liu, and Z.W. Yu, “Uncertainty analysis of the long-term deformation of CRTS III slab ballastless track-prestressed concrete simply supported girders”, *Structures*, vol. 54, pp. 1124–1136, 2023, doi: [10.1016/j.istruc.2023.05.017](https://doi.org/10.1016/j.istruc.2023.05.017).
- [6] J.Q. Cheng, X.H. Zeng, Y.K. Yang, and H.P. Gu, “Progress of filling layer of self-compacting concrete in CRTS-III type track system”, *Advanced Materials Research*, vol. 629, pp. 438–442, 2013, doi: [10.4028/www.scientific.net/AMR.629.438](https://doi.org/10.4028/www.scientific.net/AMR.629.438).
- [7] W. Jiang, Y.J. Xie, W.X. Li, and G.C. Long, “Influence of bubble defects on the bonding performance of the interlayer interface of the CRTS III slab ballastless track structure”, *Construction and Building Materials*, vol. 307, art. no. 125003, 2021, doi: [10.1016/j.conbuildmat.2021.125003](https://doi.org/10.1016/j.conbuildmat.2021.125003).
- [8] Z.P. Zeng, J.D. Wang, S.W. Shen, P. Li, A.A. Shuaibu, and W.D. Wang, “Experimental study on evolution of mechanical properties of CRTS III ballastless slab track under fatigue load”, *Construction and Building Materials*, vol. 210, pp. 639–649, 2019, doi: [10.1016/j.conbuildmat.2019.03.080](https://doi.org/10.1016/j.conbuildmat.2019.03.080).
- [9] W. Jiang, Y.J. Xie, J.X. Wu, and G.C. Long, “Influence of age on the detection of defects at the bonding interface in the CRTS III slab ballastless track structure via the impact-echo method”, *Construction and Building Materials*, vol. 265, art. no. 120787, 2020, doi: [10.1016/j.conbuildmat.2020.120787](https://doi.org/10.1016/j.conbuildmat.2020.120787).
- [10] D. Bonen and S.P. Shah, “Fresh and hardened properties of self-consolidating concrete”, *Progress in Structural Engineering and Materials*, vol. 7, no. 1, pp. 14–26, 2005, doi: [10.1002/pse.186](https://doi.org/10.1002/pse.186).
- [11] K.H. Khayat, “Workability, testing, and performance of self-consolidating concrete”, *Materials Journal*, vol. 96, no. 3, pp. 346–353, 1999, doi: [10.14359/632](https://doi.org/10.14359/632).
- [12] H. Zhao, W. Sun, X.M. Wu, and B. Gao, “The effect of sand ration on the properties of self-compacting concrete”, *Magazine of Concrete Research*, vol. 65, no. 5, pp. 275–282, 2013, doi: [10.1680/macr.11.00089](https://doi.org/10.1680/macr.11.00089).
- [13] M. Kurt, A.C. Aydın, M.S. Gül, R. Gül, and T. Kotan, “The effect of fly ash to self-compactability of pumice aggregate lightweight concrete”, *Sadhana*, vol. 40, pp. 1343–1359, 2015, doi: [10.1007/s12046-015-0337-y](https://doi.org/10.1007/s12046-015-0337-y).
- [14] B. Felekoğlu, S. Türkel, and B. Baradan, “Effect of water/cement ratio on the fresh and hardened properties of self-compacting concrete”, *Building and Environment*, vol. 42, no. 4, pp. 1795–1802, 2007, doi: [10.1016/j.buildenv.2006.01.012](https://doi.org/10.1016/j.buildenv.2006.01.012).
- [15] M. Yakhlaif, M. Safiuddin, and K.A. Soudki, “Properties of freshly mixed carbon fibre reinforced self-consolidating concrete”, *Construction and Building Materials*, vol. 46, pp. 224–231, 2013, doi: [10.1016/j.conbuildmat.2013.04.017](https://doi.org/10.1016/j.conbuildmat.2013.04.017).
- [16] T. Ponikiewski and J. Katzer, “Fresh mix characteristics of self-compacting concrete reinforced by fibre”, *Periodica Polytechnica Civil Engineering*, vol. 61, no. 2, pp. 226–231, 2017, doi: [10.3311/PPCI.9008](https://doi.org/10.3311/PPCI.9008).
- [17] M. Jalal, A. Pouladkhan, O.F. Harandi, and D. Jafari, “Comparative study on effects of Class F fly ash, nano silica and silica fume on properties of high performance self-compacting concrete”, *Construction and Building Materials*, vol. 94, no. 90, p. 104, 2015, doi: [10.1016/j.conbuildmat.2015.07.001](https://doi.org/10.1016/j.conbuildmat.2015.07.001).
- [18] Z.G. Guo, et al., “Development of sustainable self-compacting concrete using recycled concrete aggregate and fly ash, slag, silica fume”, *European Journal of Environmental and Civil Engineering*, vol. 26, no. 4, pp. 1453–1474, 2022, doi: [10.1080/19648189.2020.1715847](https://doi.org/10.1080/19648189.2020.1715847).

- [19] P. Nipat, O. Masahiro, R. Sovannasathya, and A. Anuwat, “Enhanced entrainment of fine air bubbles in self-compacting concrete with high volume of fly ash using defoaming agent for improved entrained air stability and higher aggregate content”, *Construction and Building Materials*, vol. 144, pp. 1–12, 2017, doi: [10.1016/j.conbuildmat.2017.03.049](https://doi.org/10.1016/j.conbuildmat.2017.03.049).
- [20] A. Anuwat, R. Sovannasathya, T. Kazunori, and O.C. Masahiro, “Improvement of self-compactability of air-enhanced self-compacting concrete with fine entrained air”, *Journal of Advanced Concrete Technology*, vol. 14, no. 3, pp. 55–69, 2016, doi: [10.3151/jact.14.55](https://doi.org/10.3151/jact.14.55).
- [21] H. Liu, G.C. Duan, J.Y. Zhang, and Y.H. Yang, “Rheological properties of paste for self-compacting concrete with admixtures”, *Archives of Civil Engineering*, vol. 68, no. 3, 2022, doi: [10.24425/ace.2022.141904](https://doi.org/10.24425/ace.2022.141904).
- [22] K. Ostrowski and K. Furtak, “Influence of carbon fibre reinforced polymer and recycled carbon fibres on the compressive behaviour of self-compacting high-performance fibre-reinforced concrete”, *Archives of Civil Engineering*, vol. 69, no. 2, 2023, doi: [10.24425/ace.2023.145252](https://doi.org/10.24425/ace.2023.145252).
- [23] J.B. Peng, X.H. Zeng, Z. Tang, G.H. Long, and Y.J. Xie, “Defect detection within filling layer of subway slab ballastless track based on impulse response method”, *Engineering Structures*, vol. 315, art. no. 118517, 2024, doi: [10.1016/j.engstruct.2024.118517](https://doi.org/10.1016/j.engstruct.2024.118517).
- [24] J. Wu, Z. Jia, and X. Zhou, “Discrete element analysis of the effect of aggregate morphology on the flowability of self-compacting concrete”, *Case Studies in Construction Materials*, vol. 18, art. no. e02010, 2023, doi: [10.1016/j.cscm.2023.e02010](https://doi.org/10.1016/j.cscm.2023.e02010).
- [25] L.Y. Pei, et al., “Damage and fracture investigation of self-compacting concrete in the filling layer of CRTS-III using three-point bending tests”, *Journal of Building Engineering*, vol. 89, art. no. 109285, 2024, doi: [10.1016/j.jobe.2024.109285](https://doi.org/10.1016/j.jobe.2024.109285).
- [26] M. Su, Q. Chong, H. Xie, Y.X. Xie, and Z.P. Zeng, “On the deformation of CRTS-III ballastless track during the casting process of self-compacting concrete: Numerical simulations and random forest-based prediction models”, *Engineering Structures*, vol. 307, art. no. 117870, 2024, doi: [10.1016/j.engstruct.2024.117870](https://doi.org/10.1016/j.engstruct.2024.117870).
- [27] W. Jiang, Y.J. Xie, K.L. Ma, J.Q. Wu, and G.C. Long, “Research on two-dimensional digital characterization of crushed stone aggregates in the SCC filling layer of the CRTS III slab ballastless track”, *Construction and Building Materials*, vol. 403, art. no. 133132, 2023, doi: [10.1016/j.conbuildmat.2023.133132](https://doi.org/10.1016/j.conbuildmat.2023.133132).
- [28] G.C. Long, H. Liu, K.L. Ma, Y.J. Xie, and W.G. Li, “Development of high-performance self-compacting concrete applied as the filling layer of high-speed railway”, *Journal of Materials in Civil Engineering*, vol. 30, no. 2, art. no. 04017268, 2018, doi: [10.1061/\(ASCE\)MT.1943-5533.0002129](https://doi.org/10.1061/(ASCE)MT.1943-5533.0002129)

Received: 2024-02-21, Revised: 2024-09-04